RSC Advances

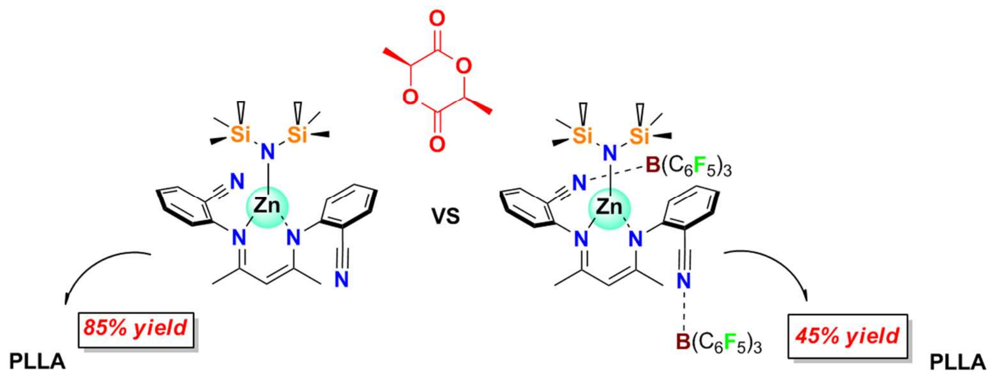

322x123mm (96 x 96 DPI)

Synthesis and Structures of *N*-Arylcyano-β-diketiminate Zinc Complexes and Adducts, their Application in Ring-Opening Polymerization of L-lactide

Oleksandra S. Trofymchuk,[a] Constantin G. Daniliuc,[b] Gerald Kehr,[b] Gerhard Erker, [b,]* and Rene S. Rojas[a,]*

Zinc amide complexes $ZnL_1N(SiMe_3)_2$, $ZnL_2N(SiMe_3)_2$ (**1** and **2**), their tris(pentafluorophenyl)borane adducts $ZnL_1N(SiMe_3)_2{\cdot}B(C_6F_5)_3$ (**3**), $ZnL_2N(SiMe_3)_2{\cdot}2B(C_6F_5)_3$ (**4**), pentafluorophenyl zinc complex $ZnL_1C_6F_5$ (**5**) and its adduct $ZnL_1C_6F_5{\cdot}B(C_6F_5)$ (**6**) supported by *N*-Arylcyano-β-diketiminate ligands, as well as bis-ligated $Zn(L_2)_2$ (**7**) were synthesized and characterized by NMR, IR, elemental analysis and X-ray diffraction. Zinc crystal structures of **1**, **4**, and **7** showed mononuclear complexes, while **2** and **5** were dimmers. ROP of L-lactide with zinc complexes and their $B(C_6F_5)_3$ adducts leads to generation of poly(L-LA) with high molecular weights and relatively narrow molecular weight distribution. The monomer conversion reached completion in 32 min only for zinc amide complex **1**, while for other compounds it was necessary to use at least 5 hours to achieve significant polymerization yields. Coordination of $B(C_6F_5)_3$ molecule close to the metal center blocks L-lactide insertion and thus decreases the activity of respective adducts in comparison with borane-free zinc complexes.

Introduction

In recent years there has been growing emphasis on the production of environmentally friendly materials. The days when the word polymer meant a resistant unbreakable material are long gone. Polylactic acid (PLA) is one of the most widely used biodegradable polymers, obtained by polymerizing lactic acid accessible from sugar. Lactide exists as three stereoisomers: L-lactide, D-lactide and *meso*-lactide. PLA can degrade by hydrolytic cleavage of the ester bonds of the polymer backbone. This property has been exploited for textiles, fibers, packaging materials, medical applications, particularly in nerve tissue engineering.[1,2] Although catalysts with various metals can polymerize lactide (Sn catalysts are used in industry for that process[3]), in the last decades the approach has been to polymerize this monomer using catalysts with non toxic and biologically benign metals, especially those with Zn.[4]

In recent years Zn catalysts capable of polymerizing L -lactide formed a large number of several families of ligands with different substituents, such as β-diketiminates, maltonates, ketiminates, bisphenolates, salycylaldiminates, and amino acids.[5] Traditional ROP initiator ligands are alkyls, amides and alkoxides. Because they are strong nucleophiles, alkoxy groups permit fast lactide ROP initiation, while amide groups require hours for that.[5c]

The substituents on the ligand affect zinc catalyst activity, structural characteristics and polydispersity of the produced PLA. Several studies have been made on how the substituents influence L -lactide polymerization.[4-9] Thus, it was shown in a series of trifluoromethyl-substituted ketones that increasing the number of electron-withdrawing groups on the ketoiminate adversely affected the stability of the zinc complexes and thereby the rate constant for lactide polymerization.[6] On the other hand, in a series of *NNO*-zinc enolate catalysts it does not seem that the difference in electronic effect of the ligands is the decisive factor for their catalytic activity.[7] In some work the effect of electron withdrawing groups in zinc catalysts is clear,[8] in others it is not.[4e,5c,6,9]

Coates and co-workers discovered that β-diketiminate zinc complexes can be used as effective lactide polymerization initiators, leading to a great increase in the development of various zinc catalysts, using different families of ligands with various substituents,[10] suggesting that a more electron-deficient zinc center would increase the CO_2/epoxide polymerization rate due to more efficient epoxide coordination Coates *et al.* investigated the influence of the addition of an electron-withdrawing cyano group to the β-diiminate ligand (Scheme 1, **A**).[10h] That resulted in the synthesis of [{Zn(μ-OMe)(BDI)}$_2$] complexes which exhibited the highest reported activity for cyclohexene oxide/CO_2 copolymerization.[10h] Other examples of zinc β-diketiminate complexes with CN groups is a highly crystalline compound **B** (Scheme 1), that form one-dimensional infinite coordination polymer chains where the CN group on the backbone of one complex links with an open coordination site of another zinc complex.[10b] Finally, Reddy *et al*. synthesized a series of CN-substituted β-diketiminate zinc complexes with a cyano group in the *para* position of the aromatic ring (Scheme 1, **C**).[11] Reported catalysts are highly active in the copolymerization of CO_2 and cyclohexene oxide. It was found that the activity of these complexes stood between the two categories reported in the literature (having no CN group and complexes having a CN group on the ligand backbone).[11]

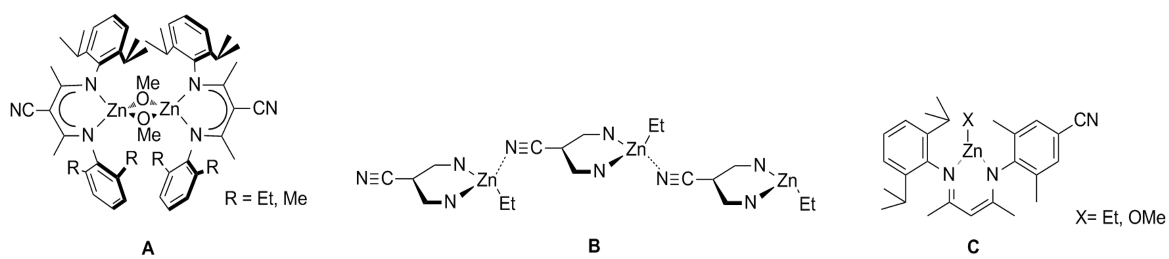

Scheme 1. Reported zinc complexes with cyano functionality in a ligand framework.

We have reported a series of *N*-arylcyano-β-diketiminate ligands with cyano groups in the *ortho* and *para* position of the aromatic ring, their methallyl nickel complexes, and the corresponding $B(C_6F_5)_3$ adducts.[12] It was found that nickel complexes alone are inactive in the polymerization or oligomerization of ethylene, while the corresponding boron adducts can activate it. The activity of boron adducts toward ethylene was strongly dependent on the hindrance near the metal center (steric factor) and $B(C_6F_5)_3$ coordinated with it (electronic factor). Inspired by these studies, we decided to synthesize a series of *N*-arylcyano-β-diketiminate zinc complexes with cyano groups in the *ortho* position of the aromatic ring, investigate their reactions with $B(C_6F_5)_3$ and $HB(C_6F_5)_2$, and their performances in the polymerization of L -lactide.

Results and discussion

Zinc amide complexes. $ZnL_1N(SiMe_3)_2$, and $ZnL_2N(SiMe_3)_2$ (**1** and **2**) were prepared by reaction of $Zn[N(SiMe_3)_2]_2$ with β-diketiminate ligands L_1H, L_2H, producing the corresponding amide complexes in 68% (**1**) and 75% (**2**) yields (Scheme 2). $^1H/^{13}C$ NMR spectroscopy is consistent with the molecular structure and *NN*-coordination of the deprotonated ligands L_1H and L_2H.

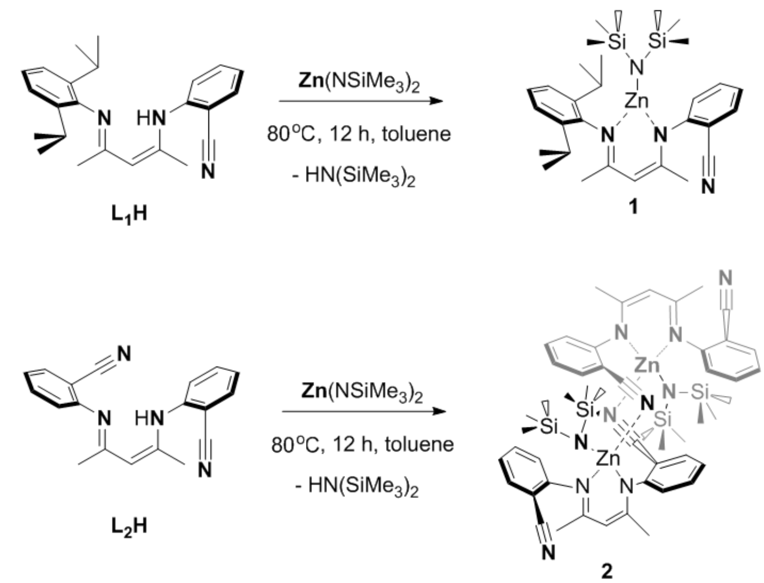

Scheme 2. Synthesis of $ZnL_1N(SiMe_3)_2$ (**1**) and $ZnL_2N(SiMe_3)_2$ (**2**).

The ^1H NMR spectra in C_6D_6 with sharp signals of **1** and **2** showed the presence of a β-diketiminate ligand and a bis(trimethylsilyl)amide. The methyl groups of trimetilsilylamide (0.03 ppm) in compound **1** are seen as a broad doublet, and their widths are due to their slow rotation caused by the steric hindrance of isopropyl groups. In compound **2**, on the other hand, the trimetilsilylamide methyl groups are seen as a sharp singlet at 0.00 ppm, indicating free rotation of this group in solution. The IR $\tilde{\nu}$(C≡N) cyano band for **1** and **2** was shifted by $\tilde{\nu}$ = 6 cm^{-1} and $\tilde{\nu}$ = 10 cm^{-1}, respectively, to higher wavenumbers compared to the L_1H and L_2H ligand systems (see Supporting Information). [12]

Crystal Structure Studies of Zinc Amide Complexes. Crystals of **1** and **2** suitable for X-ray crystallography were grown by layering pentane onto a toluene solution under an inert atmosphere at -30 °C. The crystal structure of **1** confirms the tridentate coordination of zinc by the β-diketiminate ligand and trimetilsilylamide (Figure 1). The solid state structure shows that in the zinc complex **1** the $N(SiMe_3)_2$ fragment belongs mainly to the mean ligand plane (deviation of N3 atom from the ligand plane (N1, C1, C2, C3, N2) 0.65 Å, Figure 1). Compound **1** crystallizes as a mononuclear zinc complex, while **2** crystallizes with formation of a dimer where the zinc atom coordinates with the cyano group of a neighboring ligand, thereby completing the zinc coordination number to 4 (see Figure 2). Both ligands in dimer structure **2** are *trans* with respect to each other, the Zn1- N4*-C26* angle is 159.13°, showing that the cyano group lies out of the metal center plane. Four-coordinate zinc **2** adopts a distorted tetrahedral geometry with angles larger than for an ideal environment (N3-Zn1-N4* 111.29°, N3-Zn1-N1 125.36°, N3-Zn1-N2 128.84°). The Zn···Zn nonbonding distance is 6.2733(2) Å, and the six-membered Zn_2N_4 metallacycle forms a cavity (N1*-N1 5.8033 (2) Å, N4*-N4 3.4340 (1), Figure 2). The Zn-N bond distances for complex **1** (Zn1-N1 1.971 (2), Zn1-N2 1.956 (2), Zn1-N3 1.883) are shorter than for four-coordinate dimer **2** (Zn1-N1 1.985 (2), Zn1-N2 2.000 (2), Zn1-N3 1.902). The Zn-N (amide) bond distance of 1.902 Å for **2** is a little larger than reported for β-diketiminate zinc complexes.[13] The formation of a monomer structure instead of a dimer in the case of complex **1** must be caused by steric hindrance. Complex **1** has bulky isopropyl substituents and amide group that does not allow forming a dimer and complete the coordination number of zinc to 4. For further details see Supporting Information.

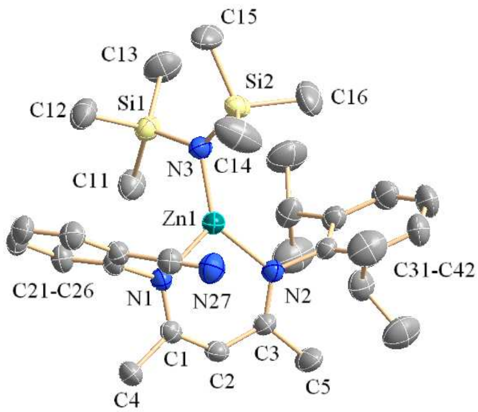

Figure 1. X-ray crystal structure of **1** with thermal ellipsoids drawn at the 50% probability level. Hydrogen atoms are omitted for clarity. Selected bond lengths (Å) and angles (deg): Zn1-N1 1.971 (2), Zn1-N2 1.956 (2), Zn1-N3 1.883 (2), N1-Zn1-N3 126.5 (1), N2-Zn1-N3 135.6 (1), N1-Zn1-N2 97.7 (1), C2-Zn1-N3 169.2 (1)

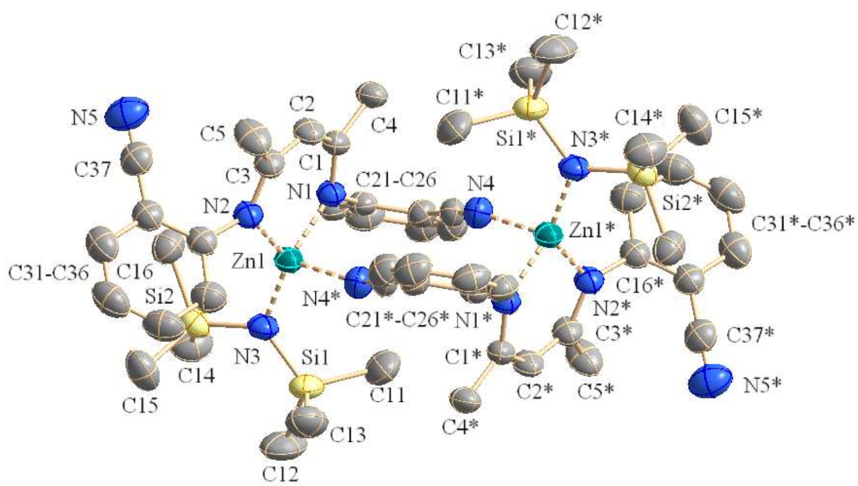

Figure 2. X-ray crystal structure of **2** with thermal ellipsoids drawn at the 50% probability level. Hydrogen atoms are omitted for clarity. Selected bond lengths (Å) and angles (deg): Zn1-N1 1.985 (2), Zn1-N2 2.000 (2), Zn1-N3 1.902 (2), Zn1-N4* 2.262 (3), Zn1- N4*-C26* 159.1 (2), N1-Zn1-N3 125.4 (1), N2-Zn1-N3 128.8 (1), N1-Zn1-N2 96.9 (1), N3-Zn1-N4* 111.3 (1)

$Zn_2(L_1)_2(OH)_2$ (1^a). Zinc amide complex **1** with a long stay in a solution (toluene) was spotted to decompose into the bimetallic zinc complex $Zn_2(L_1)_2(OH)_2$ (**1^a**). Single crystals of this compound suitable for X-ray diffraction were obtained, but only in quantities insufficient for further characterization (See supporting information, page 21).

Synthesis of $B(C_6F_5)_3$ adducts. To study the influence of remote activation[14] on the zinc amide complexes, we prepared their tris-(pentafluorophenyl)borane, $B(C_6F_5)_3$, adducts. Complexes **1** and **2** were reacted with one and two equivalents of $B(C_6F_5)_3$, and stirring the reaction mixture for 10 min at room temperature in toluene yielded borane adducts **3** and **4**, respectively, as bright yellow crystalline solids in 81 and 83% yields (Scheme 3).

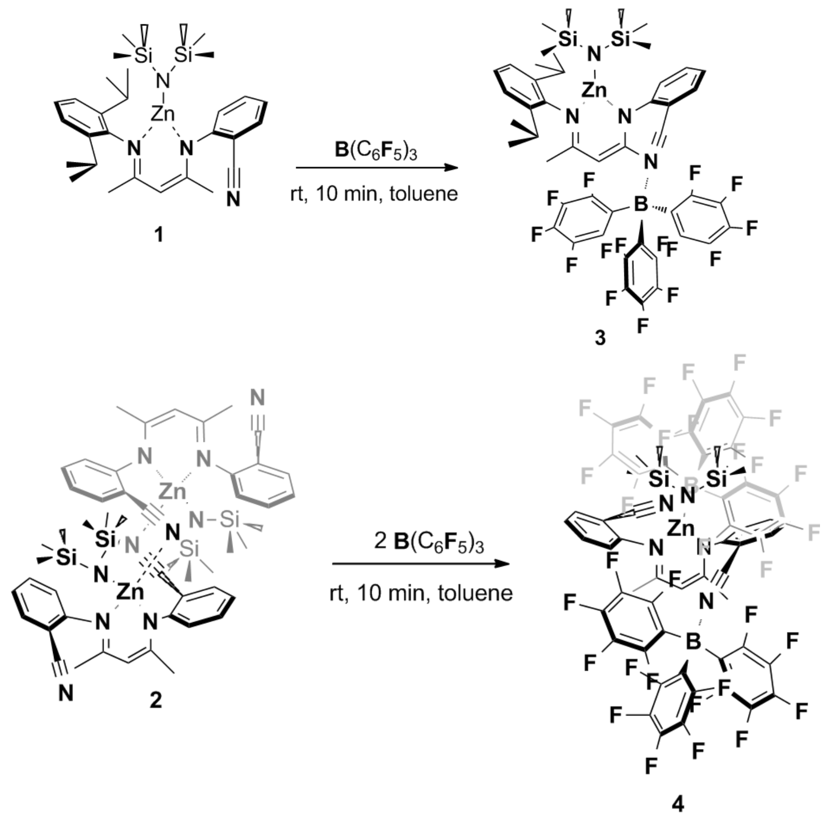

Scheme 3. Adducts **3** and **4**.

The IR $\tilde{\nu}$(CN) band is shifted very characteristically upon Lewis acid adduct formation from 2223 cm^{-1} in **1** to 2305 cm^{-1} in **3** and from 2226 cm^{-1} in **2** to 2301 cm^{-1} in **4**.[12,14] The ^{1}H NMR spectra of adducts **3** and **4** show sharp signals. The borane adduct formation in **3** and **4** is indicated by the ^{11}B NMR chemical shift of -9.74 and -8.62 ppm, respectively, characteristic of nitrile-coordinated $B(C_6F_5)_3$.[12,14] $\Delta\delta$ (p, m) values of 7.22 and 7.57 ppm in the ^{19}F NMR for compounds **3** and **4** are consistent with neutral, four-coordinate borane adducts of $B(C_6F_5)_3$.[15] Broad Ar^{F5}-*C* quaternary carbon signals in the ^{13}C NMR spectra are consistent with the $B(C_6F_5)_3$ coordination. The methyl groups of trimethylsilylamide at δ 0.11 and 0.25, isopropyl methyl and methylene protons at 1.03, 1.15, 1.25 and 2.9, 2.99 ppm in compound **3** are shifted with respect to **1** and are sharp and well defined signals due to the restricted rotation of the aromatic rings. It was not possible to obtain single crystals suitable for X-ray structure analysis for compound **3** (**1**·$B(C_6F_5)_3$·adduct).

Crystal Structure Studies of compound 4 ($B(C_6F_5)_3$ -2 adduct). Single crystals of **4** suitable for X-ray structure analysis were obtained from toluene/pentane by the diffusion method. $B(C_6F_5)_3$ coordinates with cyano groups as expected, forming a monomer structure **4** (in contrast with the dinuclear complex **2**) where both C7-N3-B1 (175.4 (4)°) angles are practically straight (Figure 3). Dihedral angles Zn1-N1-C11-C12 and Zn1-N1-C11-C16 are 105.0 (3)° and -70.4 (4)° showing that both aryl substituents are rotated out of the central plane. Interestingly, the same dihedral angles in a methallyl nickel $B(C_6F_5)_3$ adduct are about 90°.[12] Due to the presence of the bulky $N(SiMe_3)_2$ group in adduct **4**, aromatic substituents with coordinated borane were forced to take precisely this type of spatial location (Figure 3). Zn-N (β-diketiminate), Zn-N (amide) bond lengths for **4** are 1.958 (3) Å and 1.860 (4) Å, which is less than the analogous bond lengths of borane-free zinc dimer complex **2**.

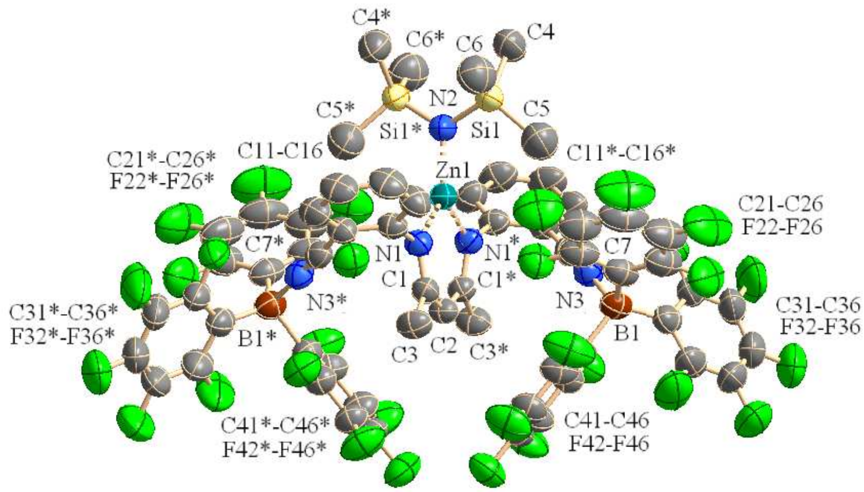

Figure 3. X-ray crystal structure of **4** with thermal ellipsoids drawn at the 50 % probability level. Hydrogen atoms are omitted for clarity. Selected bond lengths (Å) and angles (deg): Zn1-N1 1.958 (3), Zn1-N1* 1.958 (3), Zn1-N2 1.860 (4), N1-Zn1-N1* 96.6 (2), N1-Zn1-N2 131.7 (1), C7-N3-B1 175.4 (4), N1*-Zn1-N2 131.7 (1), C7-N3-B1 175.4 (4), Zn1-N1-C11-C12 105.0 (3), Zn1-N1-C11-C16 -70.438 (2)

Reaction of 1 with $HB(C_6F_5)_2$. It was decided to investigate the interaction of zinc complex **1** (one *cyano* group) with $HB(C_6F_5)_2$ (Piers' borane). $HB(C_6F_5)_2$ was previously found to successively coordinate and hydroborate the cyano group.[16] **1** was reacted with Piers' borane. Stirring the reaction mixture at room temperature in deuterated benzene solution showed the formation of the $HB(C_6F_5)_2$ adduct, where the borane molecule coordinates the nitrile group of the zinc amide complex **1** (see Figure 4, 26-40 °C, the blue circle denotes the diketiminate C*H* proton of adduct **1·$HB(C_6F_5)_2$**). The isopropyl C*H*(CH_3)$_2$ and C*H* protons at 2.92, 2.98 and 4.7 ppm in the $HB(C_6F_5)_2$ adduct are shifted with respect to the free complex **1** (Figure 4, Supporting Information, page 2). The reaction solution was heated to 70 °C and was left at this temperature for 30 minutes, then the reaction mixture was cooled to 26 °C (see Figure 4) and the formation of new compounds was observed. Among the products, one was obtained in higher yield. After evaporating of solvent, the major reaction product was purified by washing with pentane (Figure 4, the green circle denotes the diketiminate C*H* proton of the new compound). It was expected to obtain the zinc compound with a reduced nitrile group, but the absence of signals of a CH=NH functional group in the ^{1}H and ^{13}C NMR spectra, and the absence of a ^{11}B signal in boron NMR indicated that the cyano group was not hydroborated and that another main product was formed. After complete NMR analysis, the formation of $ZnL_1C_6F_5$ (**5**) was discovered (see Figure 4, Scheme 4), and it was confirmed by X-ray crystal structure analysis. It had previously been reported that alkylzinc or alkylaluminum precursors react with $B(C_6F_5)_3$ producing the corresponding pentafluorophenyl metal complexes.[17] Similarly, an interaction of $HB(C_6F_5)_2$ with zinc amide complex **1** can be assumed with these reactions. The ^{1}H NMR spectra of **5** showed the presence of β-diketiminate ligand, the isopropyl group signals at 1.23, 1.36, 3.31 and 3.45 ppm are broad, indicating the restricted rotation of the 1,3-bis(2,6-diisopropylphenyl) aromatic substituent due to the proximity of the C_6F_5 group. The IR $\tilde{\nu}$(CN) band of **5** is found at 2249 cm^{-1}, shifted with respect to zinc amide complex **1** (2225 cm^{-1}) due to the stronger electron withdrawing C_6F_5 group. $\Delta\delta$ (p, m) value of 5.92 ppm in the ^{19}F NMR and broad Ar^{F5}-*C* quaternary carbon signals in the ^{13}C NMR spectra of compound **5** are consistent with C_6F_5 ring coordination.[18]

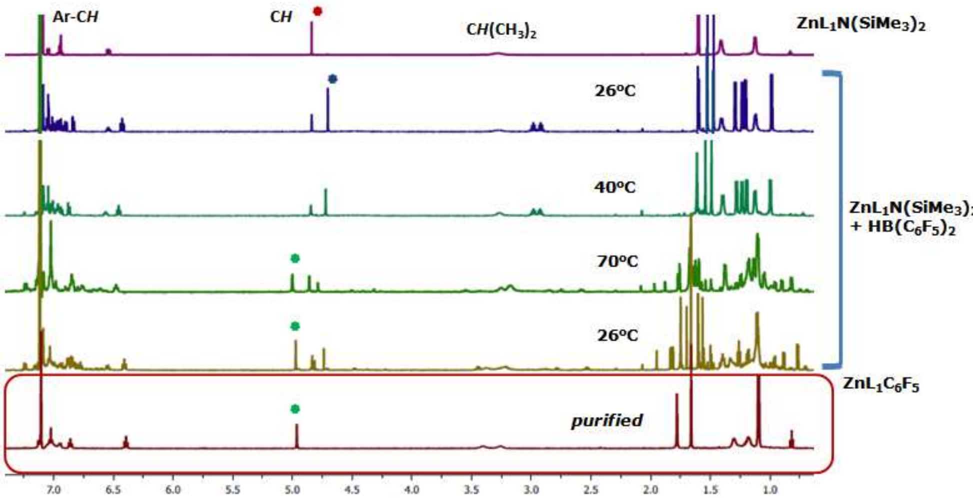

Figure 4. ^{1}H NMR spectra of the interaction between zinc complex **1** and $HB(C_6F_5)_2$. Red, blue and green dots denote the diketiminate C*H* proton of zinc complex **1**, adduct **1·HB(C$_6$F$_5$)$_2$**, and compound **5**, respectively (see Scheme 4).

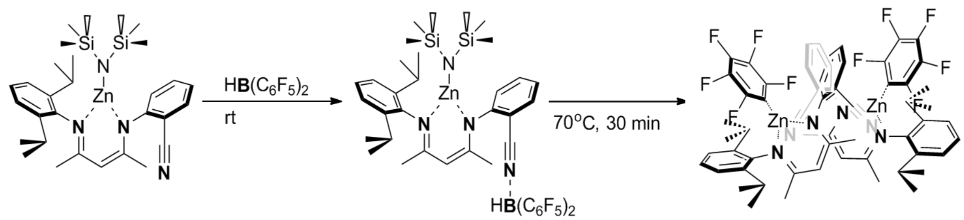

1 1·HB(C$_6$F$_5$)$_2$ 5

Scheme 4. Synthesis of **ZnL$_1$C$_6$F$_5$** (**5**).

Crystal Structure of ZnL$_1$C$_6$F$_5$ (**5**)**.** Single crystals for X-ray crystallography were grown by layering pentane onto a toluene solution of compound (**5**) at room temperature. Zinc dimer **5** is formed through coordination of the nitrile group with the neighboring zinc center, thus four-coordinate zinc in **5** adopts a distorted tetrahedral geometry (C11-Zn1-N2 121.0 (1), C21-Zn2-N4 119.8 (1), Figure 5). The Zn1-N47-C47 and Zn2-N37-C37 angles are 151.2 (4)^{o} and 149.4 (4)^{o}, more obtuse than in zinc dimer **2**. The Zn···Zn nonbonding distance is 6.198 Å and the six-membered Zn_2N_4 metallacycle forms a cavity (N47-N37 3.476 Å, see Figure 5). Zn-N bond distances for complex **5** (Zn1-N1 1.984 (3), Zn1-N2 1.972 (3), Zn2-N3 1.980 (3), Zn2-N4 1.978 (3)) are a bit longer compared to compound **1**. The Zn-N(amide) bond distances for dimer **5** are 2.121 (3) and 2.143 (3) Å, that is, longer than for **1** and the reported (DIPP)$_2$NacNacZnC$_6$F$_5$·THF (2.011 (2) Å) monomer.[19]

Synthesis of ZnL$_1$C$_6$F$_5$·B(C$_6$F$_5$)$_3$ adduct (6). Zinc complex **5** was reacted with one equiv. of $B(C_6F_5)_3$, and stirring the reaction mixture for 20 min at room temperature in toluene yielded borane adduct **6** as orange crystals in 73% yield (Scheme 5). The structure of **6** was identified by complete NMR and elemental analyses (see Supporting Information, pages 15-18). The IR $\tilde{\nu}$(CN) band is shifted from 2249 cm^{-1} in **5** to 2319 cm^{-1} in **6** upon $B(C_6F_5)_3$ coordination.[12,14] Well defined signals in the ^{1}H NMR spectrum of **6** are shifted with respect to **5**. Interestingly, the methylene proton signal of **6**

is seen as one septet (2.90 ppm), while compound **5** has two methylene proton signals (3.31, 3.45 ppm). The borane adduct formation is indicated by the ^{11}B NMR chemical shift of -9.52 ppm. In ^{19}F-^{19}F GCOSY NMR spectra signals related to $B(C_6F_5)_3$ coordinated with nitrile group and signals of C_6F_5 group coordinated with zinc were observed, with $\Delta\delta$ (p, m) values of 7.21 and 7.67 ppm, respectively, proving the formation of adduct **6**, by breakage of the zinc dimer **5**.

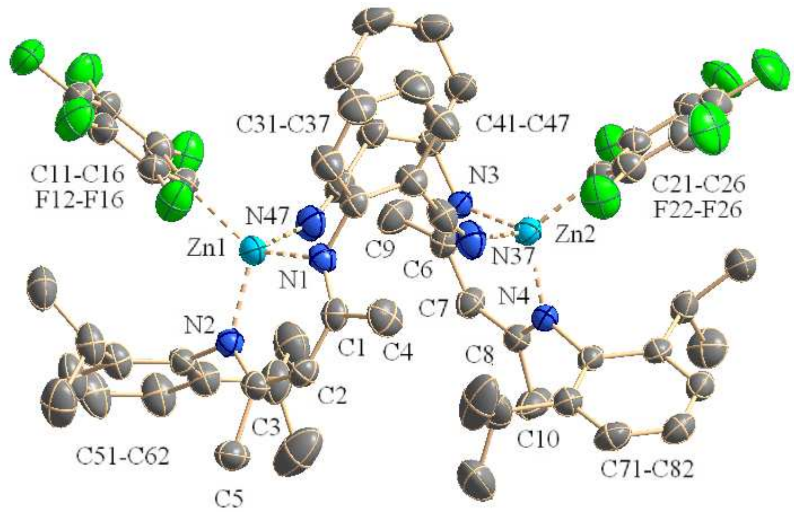

Figure 5. X-ray crystal structure of **5** with thermal ellipsoids drawn at the 50 % probability level. Hydrogen atoms are omitted for clarity. Selected bond lengths (Å) and angles (deg): Zn1-N1 1.984 (3), Zn1-N2 1.972 (3), Zn1-N47 2.143 (3), Zn1-C11 2.007 (4), Zn2-N3 1.980 (3), Zn2-N4 1.978 (3), Zn2-N37 2.121 (3), Zn2-C21 2.006 (4), Zn1-Zn2 6.198, C47-C37 3.286, N47-N37 3.476, N1-Zn1-N2 98.5 (1), C11-Zn1-N2 121.0 (1), Zn1-N47-C47 151.2 (4), C2-Zn1-C11 139.5, N4-Zn2-N3 97.8 (1), C21-Zn2-N4 119.8 (1), Zn2-N37-C37 149.4 (4), C7-Zn2-C21 140.1

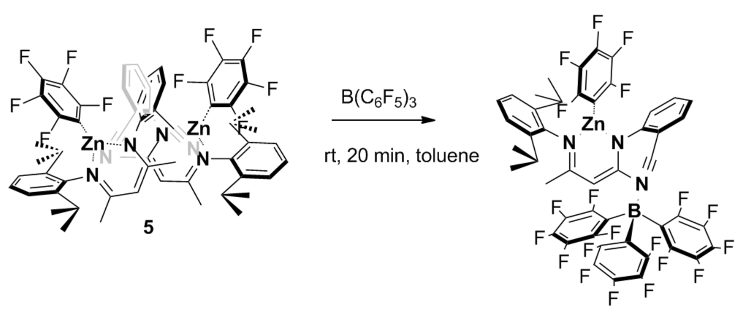

6

Scheme 5. Synthesis of $ZnL_1C_6F_5{\cdot}B(C_6F_5)_3$ (**6**).

Bis-diketiminate zinc complex. Compound $Zn(L_2)_2$ (**7**) (Scheme 6) was observed as a minor species during the synthesis of zinc amide complex **2**. At first it was difficult to identify the structure of this side product because of its complicated ^{1}H NMR spectra, with a variety of signals due to the existence of structural isomers of compound **6** in the solution (see Supporting Information, pages 18-21). Finally, zinc complex **7** was identified through its intentional synthesis by adding 1.5 equiv. of the corresponding ligand to one equiv. of $Zn\{N(SiMe_3)_2\}_2$. The ^{1}H NMR spectrum of the isolated product revealed the absence of the amide (N*H*) proton signal (*δ* 12.02 ppm) in L_2H[12] and the bis(trimethylsilyl)amide peak (*δ* 0.3 ppm). Structural isomerism in the solution of zinc complex **7** is due to the presence of 4 different cyano groups in this compound, thus the cyano groups on each aromatic ring may be *cis* or *trans* with respect to each other, giving rise to different isomers with their corresponding proton chemical shifts. For example, there are four signals corresponding to the C*H* diketiminate protons (δ 4.58, 4.63, 4.65, 4.67 ppm) in the ^{1}H NMR spectra of **7**. Curiously, by taking a proton NMR of **7**, these signals are present always in the same ratio (1:1:1.3:0.5).

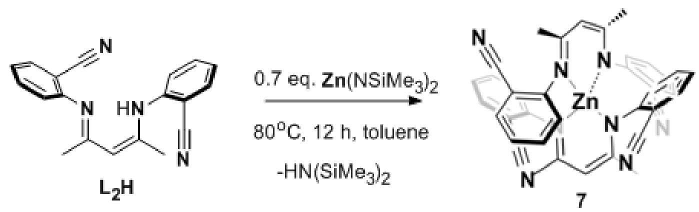

Scheme 6. Synthesis of Zn(L$_2$)$_2$ (**7**).

Crystal Structure Studies of Zn(L$_2$)$_2$ (7). Single crystals for X-ray crystallography were grown by layering pentane onto a toluene solution of compound (**7**) at -30 ^{o}C. As seen in Figure 6, the central Zn^{2+} cation is coordinated with four N atoms from each of two β-diketiminate ligands, thereby exhibiting a distorted tetrahedral geometry (See angles (deg): N1-Zn1-N3 110.1 (1), N1-Zn1-N4 119.4 (1), N1-Zn1-N2 96.5 (1), Figure 6). In one of the two coordinated β-diketiminate ligands the nitrile groups are *trans* with respect to each other, the N17-N27 distance is 8.364 Å, and the atom of zinc is in the same plane as this ligand (dihedral angles Zn1-N2-C3-C2 -9.7 (4), Zn1-N1-C1-C2 7.4 (4) are quite small). In the second coordinated β-diketiminate, the nitrile groups are *cis* with respect to each other, the N37-N47 bond distance is 3.623 Å and the dihedral angles Zn1-N3-C6-C7, Zn1-N4-C8-C7 are 17.9 (4)^o, -16.5 (4)^o respectively, resulting in a typical deviation of the ligand in complex **7** from planarity to a boat-shaped arrangement (see Figure 7).

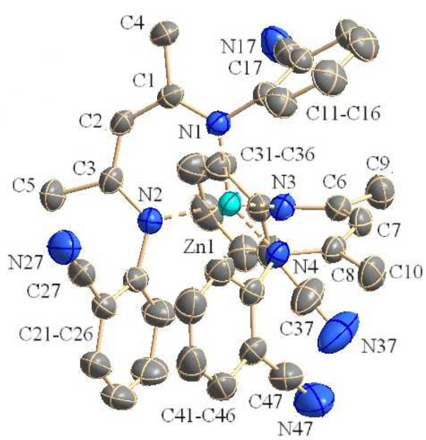

Figure 6. X-ray crystal structure of **7** with thermal ellipsoids drawn at the 50% probability level. Hydrogen atoms are omitted for clarity. Selected bond lengths (Å) and angles (deg): Zn1-N1 1.990 (2), Zn1-N2 1.954 (2), Zn1-N3 1.994 (3), Zn1-N4 1.981 (2), N17-N27 8.3643, N37-N47 3.623, N1-Zn1-N3 110.1 (1), N1-Zn1-N4 119.4 (1), N1-Zn1-N2 96.5 (1), N3-Zn1-N4 93.7 (1), Zn1-N2-C3-C2 -9.7 (4), Zn1-N1-C1-C2 7.4 (4), Zn1-N3-C6-C7 17.9 (4), Zn1-N4-C8-C7 -16.4 (4)

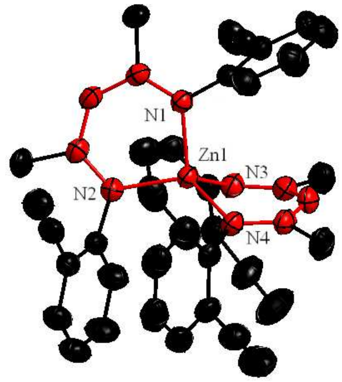

Figure 7. Side view of the slightly boat-shaped central core of zinc complex **7**.

Ring-Opening Polymerization of L-Lactide. ROP reactions were carried out at 25 and 38 °C in CH_2Cl_2 for 5 hours for compounds **2**-**7** and for 32 minutes for the zinc amide complex **1** (see Table 1, Figure 8). The total reaction volume was kept at 5 mL. The monomer/metal molar ratio used was 250. The resulting polylactides were isolated and purified by precipitation from CH_2Cl_2 with 5% HCl in methanol, followed by drying in vacuo. The molecular weights and polydispersity indices of the purified polymers were determined by size exclusion chromatography (see Experimental Part and Supporting Information). $ZnL_1N(SiMe_3)_2$ (**1**) displayed high activity at room temperature, the monomer conversion nearly reached completion after 32 min (see Entry 1). Interestingly, $[(Nacnac^{iPr})Zn(N(SiMe_3)_2)]$[20a] used in polymerization of *rac*-LA (in CH_2Cl_2 at 25 ˚C, monomer/metal molar ratio 250) displayed 97% monomer conversion after 10 hours, with an M_n value of 33.600 g/mol and polydispersity index of 2.95.[20a] In this way, the $ZnL_1N(SiMe_3)_2$ (**1**) catalyst with one cyano group in the *ortho* position of the aromatic ring proves to be more active than analogous compound with isopropyl groups only (see Table 1 and Table 2). The zinc amide catalyst $ZnL_2N(SiMe_3)_2$ (**2**) (Entry 2) proved to be less active than **1**, 85% conversion occurred after five hours, and the polydispersity index is 1.56. This is a result of the presence of two nitrile groups in **2** instead of one nitrile group in **1**. The nitrile group can compete for coordination with the zinc metal center (Figure 2) with L-Lactide, thus increasing the conversion time and favoring complex decomposition. Ligands bearing electron withdrawing groups were reported to decompose to bis-ligated zinc complexes (Scheme 6, Figure 6).[5a, 6]

Table 1. Polymerization of L-Lactide Using Zinc Complexes and Adducts (**1**-**7**).

Entry	Catalyst	[Zn]:lactide^a	Time, min	Conversión^b	T, °C
1	$ZnL_1N(SiMe_3)_2$ (**1**)	250	40	95%	25
2	$ZnL_2N(SiMe_3)_2$ (**2**)	250	300	85%	25
3	**1**·$B(C_6F_5)_3$ (**3**)	250	300	0%	38
4	**2**·$2B(C_6F_5)_3$ (**4**)	250	300	45%	38
5	$ZnL_1C_6F_5$ (**5**)	250	300	35%	38
6	$ZnL_1C_6F_5 \cdot B(C_6F_5)_3$ (**6**)	250	300	13%	38
7	$Zn(L_2)_2$ (**7**)	250	300	0%	38

^{a}All reactions were carried out in CH_2Cl_2 at 25 and 38 °C. [LA] 0.86 M in CH_2Cl_2. ^{b}Lactide conversion was determined by ^1H NMR.

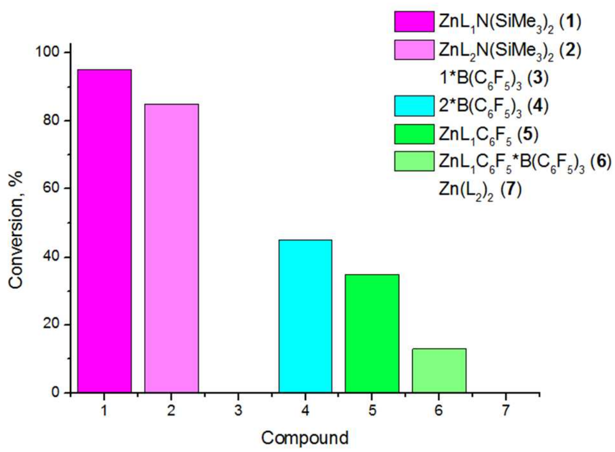

Figure 8. Monomer conversion initiated by complexes and adducts **1-7** (carried in CH_2Cl_2 at 25 °C (**1-2**) and 38 °C (**3-7**), monomer/metal molar ratio 250, [LA] 0.86 M in CH_2Cl_2, see Table 1).

In boron adducts lactide polymerization activity was reduced compared to borane free amide complexes **1** and **2**. Zinc adduct **3** (**1**·$B(C_6F_5)_3$) showed to be inactive toward L-lactide polymerization, and even when heated to 38 °C for five hours no traces of polylactide were detected. Adduct **4** (**2**·$2B(C_6F_5)_3$) under the same conditions polymerized L-Lactide with 45% conversion after 5 hours (see Entry 4, Table 1). Both zinc complex $ZnL_1C_6F_5$ (**5**) and its borane adduct $ZnL_1C_6F_5{\cdot}B(C_6F_5)$ (**6**) presented low activity toward L-lactide polymerization, 35% and 15%, respectively, even after five hours of reaction at 38 °C. The Zn(II) in species **5** and **6** may just act a Lewis acidic center for monomer activation with the nitrile (acting as a nucleophile) subsequently ring-opening the Zn-coordinated lactide. In this regard, $Zn(C_6F_5)_2$ is known to act as a strong Lewis acid in the ROP of lactide.[20b] It has been previously reported that in some instances bis-ligated complexes are active ROP catalysts,[5c, 8, 21] but $Zn(L_2)_2$ (**7**) was unable to initiate the polymerization of L-Lactide even after heating (Entry 7). Polymerization with the zinc amide complexes result in a number of processes. The primary process would be catalyst decomposition to bis-ligated complexes. The long polymerization times where complexes were in solution resulted from the low nucleophilicity and slow ROP initiation of the amide and pentafluorophenyl ligand, and as a result the number of active catalyst sites that led to polymeric materials with high molecular weights is reduced.[22, 23]

The coordination of $B(C_6F_5)_3$ molecules provides more electron deficient metal centers than those without coordinated borane.[12] Furthermore, the $B(C_6F_5)_3$ molecule is quite large, and being coordinated close to the metal center (*ortho* position of the cyano group on the catalyst's aromatic ring) it prevents L-lactide coordination (Scheme 7). This explains that adduct **3** is inactive to polymerize L-lactide, and the activity of adduct **4** is much smaller than that of **2**. $B(C_6F_5)_3$ plays the role of blocker of L-lactide insertion, thus lowering the activity of the corresponding adducts. This effect is the opposite of that present in the ethylene polymerization process, where the ethylene molecule is much smaller than the L-lactide molecule. Comparing compounds **1**, **2** with **5** and adducts **3**, **4** with **6**, the same trend is observed. It should be mentioned that the C_6F_5 group is a weaker nucleophile than $N(SiMe_3)_2$, and that explain the lower reactivity of the catalysts containing pentafluorophenyl group.

The M_n of the polymers produced by catalysts **1** and **2** increased with the monomer conversion, while the values of PDI remained relatively narrow (see Table 2, Figure 9), but not sufficient to be considered for living or quasi living polymerization. The observed and calculated molecular weights for the isolated PLLA are shown in a Table 2. The differences between M_c and M_n values can be associated to non-living character of these systems and the long polymerization times where the amides were in solution at ambient temperature resulted from the low nucleophilicity and slow ROP initiation of the amide ligand.[5c] As a result, the number of active catalyst sites was reduced.

Table 2. Polymerization of L-Lactide Using Zinc Complexes (**1-2**).

Entry[a]	**Catalyst**[b]	**Time, min**	**Conversión**[c]	**M_c (g mol^{-1})**[d]	**M_n (g mol^{-1})**[e]	**M_w/M_n**
1	$ZnL_1N(SiMe_3)_2$ (**1**)	13	59	21.000	33.000	1.7
2	$ZnL_1N(SiMe_3)_2$ (**1**)	27	89	32.000	56.000	2.0
3	$ZnL_1N(SiMe_3)_2$ (**1**)	40	95	36.000	57.000	2.6
5	$ZnL_2N(SiMe_3)_2$ (**2**)	180	69	25.000	56.000	1.6
6	$ZnL_2N(SiMe_3)_2$ (**2**)	240	79	28.000	60.000	1.5
7	$ZnL_2N(SiMe_3)_2$ (**2**)	300	85	31.000	67.000	1.6

[a]All reactions were carried out in CH_2Cl_2 at 25 °C. [b][LA] 0.86 M in CH_2Cl_2. [c]Lactide conversion was determined by ^{1}H NMR. [d]$Mc = (144.13) \times [M]_0/[I]_0 \times$ conversion. [e]Measured by SEC with PS standard calibration.

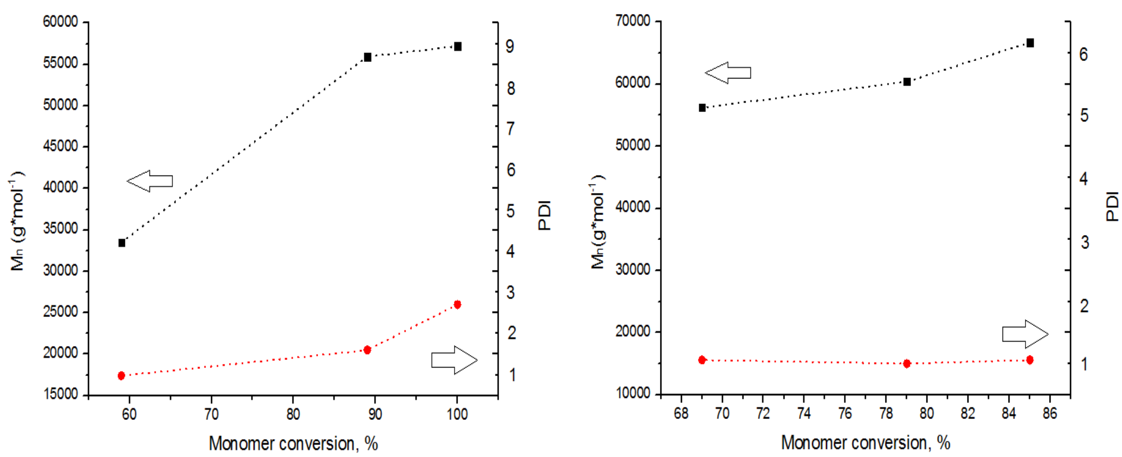

Figure 9. Polymerization of L-lactide initiated by complex **1** (left) and by complex **2** (right) in CH_2Cl_2 at 25 °C. Relationship between the number averaged molecular weight (M_n) and monomer conversion.

The end group analysis of the oligomer of PLLA, which was quenched by MeOH, was determined by ^{1}H NMR (see Supporting Information, page 27). The ^{1}H NMR spectrum exhibited the quartet characteristic of a -CH-(Me)OH terminal group at δ 4.3 ppm (this result was consistent with MALDI-TOF, see Supporting Information, page 28). The -CH-(Me)OH group was formed by hydrolysis of the Zn-N($SiMe_3$)$_2$ bond. These results indicate that the present polymerization could be supposed to proceed by a coordination insertion mechanism (see Scheme 7).

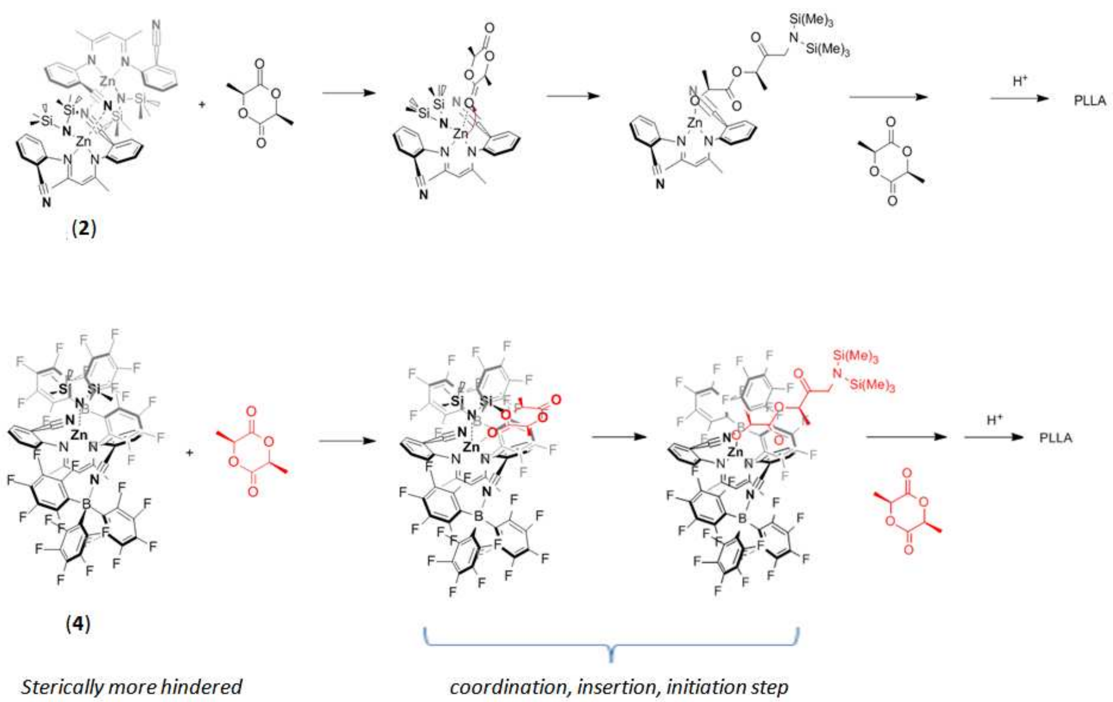

Scheme 7. Proposed mechanism for the ROP of L-lactide for zinc amide complex **2** and its $B(C_6F_5)_3$ adduct **4**.

Conclusions

Zinc amide complexes were prepared with bidentate *N*-arylcyano-β-diketiminate ligands bearing the nitrile group in the *ortho* position of the aromatic ring. The coordination of tris(pentafluorophenyl)borane with the cyano group of complexes **1** and **2** yielded borane adducts **3** and **4**. Stirring the reaction mixture of **1** at room temperature showed the formation of the $HB(C_6F_5)_2$ adduct, where the borane molecule coordinates the nitrile group of the zinc amide complex. Subsequent heating of the reaction solution resulted in the formation of zinc complex $ZnL_1C_6F_5$ (**5**), which was reacted with one equiv. of $B(C_6F_5)_3$, yielding adduct **6**. Formation of bis-ligated zinc complex $Zn(L_2)_2$ (**7**) was observed during the synthesis of zinc complex **2** and was identified through its intentional synthesis. The zinc complexes displayed good activity towards the ROP of L-LA, in contrast with borane adducts, where coordination of $B(C_6F_5)_3$ molecule close to the metal center affects the ROP. This explains the inactivity of adduct **3** to polymerize L-lactide, the activity of adduct **4** is much smaller than that of **2**, and the activity of zinc adduct **6** is lower than that of borane-free zinc complex **5**. $B(C_6F_5)_3$ plays the role of blocker of L-lactide insertion. Interestingly, the $ZnL_1N(SiMe_3)_2$ (**1**) catalyst with one cyano group in the *ortho* position of the aromatic ring proves to be more active in the polymerization of L-lactide than analogous compound [(*Nacnac*^{iPr})Zn(N(SiMe$_3$)$_2$)][20a] with isopropyl groups only.

Experimental part

General

All manipulations were performed under an inert atmosphere using standard glovebox and Schlenk-line techniques. All reagents were used as received from Aldrich, unless otherwise specified. Toluene, THF, and pentane were distilled from benzophenone ketyl. Bis-(pentafluorophenyl)borane ($HB(C_6F_5)_2$) was prepared as described in the literature.[16c] NMR spectra were recorded on VNMRS 500 MHz (Agilent), DD2 600 MHz (Agilent), Bruker AV 400, and Bruker DPX 300 spectrometers. Chemical shifts are given in parts per million relative to solvents [^{1}H and ^{13}C, δ($SiMe_4$) = 0] or an external standard [δ ($BF_3{\cdot}OEt_2$) = 0 for ^{11}B NMR, δ($CFCl_3$) = 0 for ^{19}F NMR]. Most NMR assignments were supported by additional 2D experiments. Elemental analysis data were recorded on a Foss-Heraeus CHNO-Rapid analyzer. For ESI mass spectra characterization Bruker Daltonics Micro Tof was used. Infrared spectroscopy: Varian 3100 FT-infrared spectroscopy (Excalibur Series) spectrometer. For X-ray crystal structure analysis, data sets were collected with a Nonius Kappa CCD diffractometer by Dr. Constantin G. Daniliuc; full details can be found in the independently deposited crystallography information files (cif). Graphics show thermal ellipsoids at the 50% probability level. Size exclusion chromatography (SEC) was carried out with THF as eluent at a flow rate of 1.0 mL/min at rt on a system consisting of an HPLC Pump (Knauer 14163), a set of three PLgel 5 µm MIXED-C columns and a Wyatt Technology Corporation model Dawn EOS differential refractometer detector. Data were analyzed with Astra 6.0 software based on calibration curves built upon polystyrene standards (to determine the molecular weight of polymers) with peak molecular weights ranging from 500 to 146000 g/mol. Mass spectra of PLLA were carried out using Matrix-assisted laser desorption ionizatione time of flight (MALDI-TOF). Mass spectra were recorded on a Bruker Ultraflex system equipped with a pulsed nitrogen laser (337 nm) (Bruker Daltonics Inc., Bremen Germany), operating in positive ion reflector mode, using a 19 kV acceleration voltage and a matrix of dithranol.

Synthesis of $ZnL_1N(SiMe_3)_2$ (1) $Zn\{N(SiMe_3)_2\}_2$ (128.9 mg, 278.1 mmol) and L_1H (100 mg, 278.1 mmol) were dissolved in toluene and stirred at 80 ^{o}C for 12 h. Evaporation of the solvent yielded a pale yellow, air-sensitive solid, that was washed with 3-4 ml cold pentane, and dried *in vacuo*. Yield: 110 mg (188.3 mmol, 68 %). Single crystals for X-ray crystallography were grown by layering pentane onto a toluene solution of compound (**1**) at -30 ^{o}C. ^{1}H NMR (600 MHz, C_6D_6, 299 K): δ/ppm = 0.03 (bd, 18H, N(Si*Me*$_3$)$_2$), 1.16 (d, J = 1.16 Hz, 6H, CH(C*H*$_3$)$_2$), 1.46 (d, 6H, J = 1.16 Hz, CH(C*H*$_3$)$_2$), 1.64 (s, 3H, *Me*), 1.65 (s, 3H, *Me*), 3.33 (bs, 2H, C*H*(CH$_3$)$_2$), 4.88 (s, 1H, C*H*), 6.59 (m, 1H, Ar-*H*), 6.99 (m, 2H, Ar-*H*), 7.09 (m, 1H, Ar-*H*), 7.13 (m, 3H, Ar-*H* [j,j,k]). ^{13}C {^{1}H} NMR (100 MHz, C_6D_6, 299 K): δ/ppm = 5.22 (N(Si(*C*H$_3$)$_3$)$_2$), 23.58 (CH(*C*H$_3$)$_2$), 24.51 (CH(*C*H$_3$)$_2$), 24.79 (*Me*), 28.77 (*C*H(CH$_3$)$_2$), 97.22 (*C*H), 110.77 (Ar-*C*), 117.67 (*C*≡N), 125.34 (Ar-*CH*), 126.98 (Ar-*CH*), 127.59 (Ar-*CH*), 128.06 (Ar-*C*), 128.51 (Ar-*C*), 133.05 (Ar-*CH*), 133.13 (Ar-*CH*), 143.87 (Ar-*C*), 152.59 (Ar-*C*), 167.01 (*C*=N), 171.69 (*C*=N). IR (KBr): ν/cm^{-1} = 2225 (ν (C≡N), s).

Synthesis of $ZnL_2N(SiMe_3)_2$ (2) $Zn\{N(SiMe_3)_2\}_2$ (154.3 mg, 332.9 mmol) and L_2H (100 mg, 332.9 mmol) were dissolved in toluene and stirred at 80 ^{o}C for 12 h. Evaporation of the solvent yielded a yellow, air-sensitive solid, that was washed with 5 ml cold pentane, and dried *in vacuo*. Yield: 131 mg (249.5 mmol, 75 %). Single crystals for X-ray crystallography were grown by layering pentane onto a toluene solution of compound (**2**) at -30 ^{o}C. ^{1}H NMR (600 MHz, C_6D_6, 299 K): δ/ppm = 0.00 (s, 18H, N(Si*Me*$_3$)$_2$), 1.59 (s, 6H, *Me*), 4.85 (s, 1H, C*H*), 6.54 (m, 2H, Ar-*CH*), 6.70 (m, 2H, Ar-*CH*), 6.89 (m, 2H, Ar-*CH*), 7.09 (m, 2H, Ar-*CH*). ^{13}C {^{1}H} NMR (100 MHz, C_6D_6, 299 K): δ/ppm = 5.24 (N(Si(*C*H$_3$)$_3$)$_2$), 23.73 (*Me*), 97.76 (*C*H), 110.15 (Ar-*C*), 117.42 (*C*≡N), 125.59 (Ar-*C*H), 126.67 (Ar-*C*H), 126.98 (Ar-*C*), 126.79 (Ar-*C*), 133.02 (Ar-*C*H), 133.38 (Ar-*C*H), 151.86 (Ar-*C*), 169.13 (*C*=N). IR (KBr): ν/cm^{-1} = 2226 (ν (C≡N), s).

Synthesis of $ZnL_1N(SiMe_3)_2 \cdot B(C_6F_5)_3$ (3) 1 eq of Tris(pentafluorophenyl)borane (17.6 mg in 2 mL of toluene, 34.2 mmol) was added to a toluene solution of **1** (20 mg, 34.2 mmol). The reaction mixture was stirred for 10 min, filtered and dried several hours under vacuum. Compound **3** was isolated as bright yellow solid in 81 % yield. ^{1}H NMR (600 MHz, C_6D_6, 299 K): δ/ppm = 0.11 (s, 9H, N(Si*Me*$_3$)$_2$), 0.25 (s, 9H, N(Si*Me*$_3$)$_2$), 1.03 (d, J = 1.14 Hz, 3H, CH(C*H*$_3$)$_2$), 1.15 (d, J = 1.14 Hz, 3H, CH(C*H*$_3$)$_2$), 1.25 (m, 6H, CH(C*H*$_3$)$_2$), 1.50 (s, 3H, *Me*), 1.63 (s, 3H, *Me*), 2.9 (s, 1H, C*H*(CH$_3$)$_2$), 2.99 (s, 1H, C*H*(CH$_3$)$_2$), 4.83 (s, 1H, C*H*), 6.50 (m, 1H, Ar-C*H*^{d}), 6.85 (m, 1H, Ar-C*H*), 6.95 (m, 1H, Ar-C*H*), 7.05 (m, 2H, Ar-C*H*), 7.10 (m, 1H, Ar-C*H*), 7.38 (m, 1H, Ar-C*H*^{e}). ^{13}C {^{1}H} NMR (100 MHz, C_6D_6, 299 K): δ/ppm = 4.61 (N(Si*Me*$_3$)$_2$), 5.47(N(Si*Me*$_3$)$_2$), 23.04 (*Me*), 24.23 (*Me*), 24.53 (CH(C*H*$_3$)$_2$), 24.57 (CH(C*H*$_3$)$_2$), 24.70 (CH(*C*H$_3$)$_2$), 24.77 (CH(*C*H$_3$)$_2$), 28.52 (*C*H(CH$_3$)$_2$), 28.72 (*C*H(CH$_3$)$_2$), 97.73 (*C*H), 103.72 (Ar-*C*), 115.32 (*C*≡N), 124.49 (Ar-*C*H), 124.87 (Ar-*C*H), 126.04 (Ar-*C*H^d), 127.28 (Ar-*C*H), 128.95 (Ar-*C*H), 135.53 (Ar-*C*H^e), 137.04 (Ar^{F5}-*C*), 137.89 (Ar-*C*H), 138.56 (Ar^{F5}-*C*), 140.13 (Ar^{F5}-*C*), 141.02 (Ar-*C*), 141.79 (Ar^{F5}-*C*), 142.35 (Ar-*C*), 142.87 (Ar-*C*), 147.78 (Ar^{F5}-*C*), 149.40 (Ar^{F5}-*C*), 154.83 (Ar-*C*), 165.02 (*C*=N), 173.85 (*C*=N). IR (KBr): ν/cm^{-1} = 2305 (ν (C≡N), s).

Synthesis of $ZnL_2N(SiMe_3)_2 \cdot 2B(C_6F_5)_3$ (4) 2 eq of Tris(pentafluorophenyl)borane (39 mg in 1 mL of toluene, 76.2 mmol) was added to a toluene solution of **2** (20 mg, 38 mmol). The reaction mixture was stirred for 10 min, filtered and dried several hours under vacuum. Compound **4** was isolated as bright yellow solid in 83 % yield. Single crystals for X-ray crystallography were grown by layering pentane onto a toluene solution of compound (**4**) at -30 ^{o} C. ^{1}H NMR (600 MHz, C_6D_6, 299 K): δ/ppm = 0.33 (s, 18H, N(Si*Me*$_3$)$_2$), 1.50 (s, 6H, *Me*), 4.57 (s, 1H, C*H*), 6.48 (m, 2H, Ar-*CH*^{b}), 6.95 (m, 4H, Ar-*CH*^{c,d}), 7.23 (m, 2H, Ar-*CH*^{e}).^{13}C {^{1}H} NMR (100 MHz, C_6D_6, 299 K): δ/ppm = 4.85 (N(Si(CH$_3$)$_3$)$_2$), 23.38 (*Me*), 98.51 (*C*H), 114.48 (*C*≡N), 115.48 (Ar-*C*), 127.34 (Ar-*C*H^b), 127.87 (Ar-*C*), 128.51 (Ar-*C*), 135.28 (Ar-*C*H^e), 137.09 (Ar^{F5}-*C*), 138.63 (Ar-*C*H), 138.71 (Ar^{F5}-*C*), 140.24 (Ar^{F5}-*C*), 141.93 (Ar^{F5}-*C*), 147.96 (Ar^{F5}-*C*), 149.70 (Ar^{F5}-*C*), 153.88 (Ar-*C*), 170.38 (*C*=N). IR (KBr): ν/cm^{-1} = 2301 (ν (C≡N), s).

Synthesis of $ZnL_1C_6F_5$ (5) $ZnL_1N(SiMe_3)_2$ (**1**) (50 mg, 85.6 mmol) and $HB(C_6F_5)_2$ (29.6 mg, 85.6 mmol) were dissolved in toluene and stirred at 80 ^{o} C for 12 h. The color of the solution was changed from yellow to orange. Evaporation of the solvent yielded pale orange, air-sensitive solid, that was washed several times with 2 ml cold pentane, and dried few hours under vacuum. Yield: 23.3 mg (39.4 mmol, 46 %). Single crystals for X-ray crystallography were grown by layering pentane onto a toluene solution of compound (**5**) at room temperature. ^{1}H NMR (600 MHz, C_6D_6, 299 K): δ/ppm = 1.14 (d, J = 1.15 Hz, 6H, CH(C*H*$_3$)$_2$), 1.23 (bs, 3H, CH(C*H*$_3$)$_2$), 1.36 (bs, 3H, CH(C*H*$_3$)$_2$), 1.72 (s, 3H, *Me*), 1.83 (s, 3H, *Me*), 3.31 (bs, 2H, C*H*(CH$_3$)$_2$), 3.45 (bs, 2H, C*H*(CH$_3$)$_2$), 5.02 (s, 1H, C*H*), 6.45 (t, 1H, Ar-*H*^{d}), 6.91 (t, 1H, Ar-*H*^{c}), 7.00 (d, 1H, Ar-*H*^{b}), 7.08 (m, 3H, Ar-*H*^{j,k}), 7.18 (d, 1H, Ar-*H*^{e}). ^{13}C {^{1}H} NMR (100 MHz, C_6D_6, 299 K): δ/ppm = 23.21 (*Me*), 23.69 (*Me*), 23.81 (CH(*C*H$_3$)$_2$), 24.01 (CH(*C*H$_3$)$_2$), 24.31 (CH(*C*H$_3$)$_2$), 25.07 (CH(*C*H$_3$)$_2$), 28.28 (*C*H(CH$_3$)$_2$), 28.40 (*C*H(CH$_3$)$_2$), 96.71 (*C*H), 107.71 (Ar-*C*), 117.82 (*C*≡N), 124.02 (Ar-*C*H ^{j,k}), 124.80 (Ar-*C*H^d), 126.44 (Ar-*C*H^b), 127.10 (Ar-*C*), 128.19 (Ar-*C*), 133.61 (Ar-*C*H^e), 134.62 (Ar-*C*H^c), 135.88 (Ar^{F5}-*C*), 137.65 (Ar^{F5}-*C*), 139.32 (Ar^{F5}-*C*), 140.91 (Ar^{F5}-*C*), 141.68 (Ar-*C*), 142.14 (Ar-*C*), 144.01 (Ar-*C*), 148.28 (Ar^{F5}-*C*), 149.77 (Ar^{F5}-*C*), 154.70 (Ar-*C*), 165.00 (*C*=N), 170.03 (*C*=N). IR (KBr): ν/cm^{-1} = 2249 (ν (C≡N), s).

Synthesis of $ZnL_1C_6F_5 \cdot B(C_6F_5)_3$ (6) 1 eq of Tris(pentafluorophenyl)borane (33.8 mg in 1 mL of toluene, 66 mmol) was added to a toluene solution of **6** (40 mg, 66 mmol). The reaction mixture was stirred for 20 min, filtered, washed with 3 ml cold pentane and dried under vacuum. Compound **6** was isolated as orange solid in 73 % yield. ^{1}H NMR (600 MHz, C_6D_6, 299 K): δ/ppm = 1.05 (d, J = 1.05 Hz, 3H, CH(C*H*$_3$)$_2$), 1.09 (d, J = 1.08 Hz, 3H, CH(C*H*$_3$)$_2$), 1.14 (d, J = 1.14 Hz, 3H, CH(C*H*$_3$)$_2$), 1.19 (d, J = 1.18 Hz, 3H, CH(C*H*$_3$)$_2$), 1.51 (s, 3H, *Me*), 1.63 (s, 3H, *Me*), 2.90 (s, 1H, C*H*(CH$_3$)$_2$), 5.00 (s, 1H, C*H*), 6.33 (t, 1H, Ar-*H*^{d}), 6.39 (d, 1H, Ar-*H*^{b}), 6.72 (t, 1H, Ar-*H*^{c}), 7.00 (m, 2H, Ar-*H*^{i,j}), 7.04 (m, 1H, Ar-*H*^{k}), 7.12 (d, 1H, Ar-H^e). $^{13}C\{^1H\}$ NMR (100 MHz, C_6D_6, 299 K): δ/ppm = 23.58 (*Me*), 23.60 ($CH(CH_3)_2$), 23.65 ($CH(CH_3)_2$), 23.82 ($CH(CH_3)_2$), 24.11 ($CH(CH_3)_2$), 28.67 ($CH(CH_3)_2$), 28.78 ($CH(CH_3)_2$), 98.16 (*C*H), 103.95 (Ar-C^f), 113.94 (*C*≡N), 124.17 (Ar-CH^j), 124.78 (Ar-CH^i), 126.27 (Ar-CH^d), 127.30 (Ar-CH^k), 127.59 (Ar-CH^b), 134.45 (Ar-CH^e), 137.01 (Ar^{F5}-*C*), 137.71 (Ar-CH^c), 138.65 (Ar^{F5}-*C*), 140.24 (Ar^{F5}-*C*), 140.65 (Ar-C^i), 141.84 (Ar-C^i), 141.89 (Ar^{F5}-*C*), 142.31 (Ar-C^h), 147.97 (Ar^{F5}-*C*), 149.44 (Ar^{F5}-*C*), 155.45 (Ar-C^a), 165.89 (*C*=N), 173.69 (*C*=N). IR (KBr): ν/cm^{-1} = 2319 (ν (C≡N), s).

Synthesis of $Zn(L_2)_2$ (7) Diketimine L_2H (40 mg, 133.2 mmol) and $Zn\{N(SiMe_3)_2\}_2$ (34.2 mg, 88.8 mmol) were reacted in toluene (5 ml) for 12 hours at 80 °C. The residue obtained after evaporation of the solvent was washed with pentane and dried under vacuum to yield yellow powder of **7** (36.5 mg, 62 %). Single crystals for X-ray crystallography were grown by layering pentane onto a toluene solution of compound (**7**) at -30 °C. ^1H NMR (600 MHz, C_6D_6, 299 K): δ/ppm = 1.54 (s, 6H, *Me*), 1.55 (s, 3H, *Me*), 1.57 (s, 6H, *Me*), 1.68 (s, 18H, *Me*), 1.69 (s, 6H, *Me*), 1.82 (s, 3H, *Me*), 1.98 (s, 6H, *Me*), 4.58 (s, 1H, C*H*), 4.63 (s, 3H, C*H*), 4.65 (s, 2H, C*H*), 4.67 (s, 2H, C*H*), 6.51 (m, 2H, Ar-*H*), 6.53 (m, 3H, Ar-*H*), 6.54 (m, 3H, Ar-*H*), 6.55 (m, 1H, Ar-*H*), 6.56 (m, 4H, Ar-*H*), 6.58 (m, 2H, Ar-*H*), 6.59 (m, 1H, Ar-*H*), 6.63 (m, 1H, Ar-*H*), 6.64 (m, 1H, Ar-*H*), 6.71 (m, 1H, Ar-*H*), 6.72 (m, 1H, Ar-*H*), 6.75 (m, 1H, Ar-*H*), 6.76 (m, 1H, Ar-*H*), 6.78 (m, 1H, Ar-*H*), 6.79 (m, 1H, Ar-*H*), 6.88 (m, 1H, Ar-*H*), 6.90 (m, 1H, Ar-*H*), 6.91 (m, 1H, Ar-*H*), 6.92 (m, 1H, Ar-*H*), 6.95 (m, 1H, Ar-*H*), 6.96 (m, 3H, Ar-*H*), 6.98 (m, 2H, Ar-*H*), 7.02 (m, 2H, Ar-*H*), 7.07 (m, 5H, Ar-*H*), 7.09 (m, 5H, Ar-*H*), 7.10 (m, 1H, Ar-*H*), 7.11 (m, 1H, Ar-*H*), 7.13 (m, 2H, Ar-*H*), 7.15 (m, 2H, Ar-*H*), 7.17 (m, 2H, Ar-*H*), 7.18 (m, 1H, Ar-*H*), 7.19 (m, 1H, Ar-*H*), 7.21 (m, 1H, Ar-*H*), 7.22 (m, 1H, Ar-*H*), 7.29 (m, 2H, Ar-*H*), 7.37 (m, 1H, Ar-*H*), 7.45 (m, 1H, Ar-*H*), 7.91 (m, 2H, Ar-*H*). $^{13}C\{^1H\}$ NMR (100 MHz, C_6D_6, 299 K): δ/ppm = 22.66 (*Me*), 22.71 (*Me*), 23.12 (*Me*), 23.45 (*Me*), 23.52 (*Me*), 98.27 (*C*H), 98.45 (*C*H), 98.52 (*C*H), 98.53 (*C*H), 107.99 (Ar-*C*), 108.39 (Ar-*C*), 108.40 (Ar-*C*), 109.13 (Ar-*C*), 109.19 (Ar-*C*), 116.48 (*C*≡N), 117.08 (*C*≡N), 117.6 (*C*≡N), 117.72 (*C*≡N), 118.00 (*C*≡N), 118.20 (*C*≡N), 123.35 (Ar), 123.48 (Ar-*C*H), 123.61 (Ar), 124.09 (Ar-*C*H), 124.18 (Ar), 124.24 (Ar), 124.35 (Ar), 125.00 (Ar-*C*H), 125.34 (Ar), 125.51 (Ar), 126.11 (Ar), 126.72 (Ar-*C*H), 126.78 (Ar), 127.21 (Ar), 132.17 (Ar-*C*H), 132.55 (Ar), 132.76 (Ar), 132.87 (Ar), 132.92 (Ar), 132.97 (Ar), 133.01 (Ar), 133.06 (Ar), 133.14 (Ar-*C*H), 133.32 (Ar-*C*H), 133.53 (Ar), 133.64 (Ar), 133.68 (Ar-*C*H), 135.12 (Ar), 151.62 (Ar), 152.07 (Ar), 152.88 (Ar), 153.05 (Ar), 153.29 (Ar), 153.48 (Ar), 167.39 (*C*=N), 167.53 (*C*=N), 168.04 (*C*=N), 168.45 (*C*=N), 169.07 (*C*=N), 169.71 (*C*=N), 169.84 (*C*=N). IR (KBr): ν/cm^{-1} = 2226 (ν (C≡N), s).

General procedure for lactide polymerization

In a typical polymerization reaction: under an inert atmosphere L-LA (4.3 mmol) in CH_2Cl_2 (4 mL) solution was added while stirring to a zinc compound (17.1 μmol) solution in CH_2Cl_2 (1 mL). The schlenk was placed in an oil bath if necessary at 38 °C. The solution was stirred for 5 hours for compounds **2-7** and for 32 minutes for the zinc amide complex **1**. The resulting polylactides were isolated and purified by precipitation from CH_2Cl_2 with 5% HCl in methanol, followed by drying in vacuo. The polymerization conversion was analyzed by ^1H NMR spectroscopic studies.

Acknowledgements

Authors thank Maximiliano Pino and Dr. Angel Leiva for SEC measurements. Authors thank Dr. Leonardo Silva Santos for MALDI-TOF measurement. Financial support from FONDECYT 1130077 and ICM 120082 (to R. S. R.). O.S.T. acknowledges VRI from Pontificia Universidad Catolica de Chile and Ph.D. CONICYT fellowship.

Notes and references

[a] Departamento de Quimica Inorganica, Facultad de Quimica, Pontificia Universidad Catolica de Chile, Casilla 306, Santiago-22, Chile

[b] Organisch-Chemisches Institut, Westfälische Wilhelms-Universitat, Corrensstrasse 40, D-48149 Münster, Germany

Electronic Supplementary Information (ESI) available: [details of any supplementary information available should be included here]. See DOI: 10.1039/b000000x/

1 A. B. Biernesser, B. Li and J. A. Byers, *J. Am. Chem. Soc.*, 2013, **135**, 16553-16560.

2 (*a*) N. E. Zander, J. A. Orlicki, A. M. Rawlett, and T. P. Beebe, *Jr. Appl. Mater. Interfaces,* 2012, **4**, 2074-2081; (*b*) J.-C. Buffet, A. N. Martin, M. Kol and J. Okuda, *Polym. Chem.*, 2011, **2**, 2378-2384; (*c*) A. Sauer, A. Kapelski, C. Fliedel, S. Dagorne, M. Kol and J. Okuda, *Dalton Trans.*, 2013, **42**, 9007-9023; (*d*) A. Kapelski and J. Okuda, *J. Polym. Sci. A Polym. Chem.*, 2013, **51**, 4983-4991; (*e*) J. P. Davin, J.-C. Buffet, T. P. Spaniol and J. Okuda, *Dalton Trans*., 2012, **41**, 12612-12618.

3 (*a*) D. Pospiech, H. Komber, D. Jehnichen, L. Haussler, K. Eckstein, H. Scheibner, A. Janke, H. R. Kricheldorf and O. Petermann, *Biomacromolecules*, 2005, **6**, 439-446; (*b*) E. Ruckenstein and Y. J. Yuan, *Appl. Polym. Sci.,* 1998, **69**, 1429-1434; (*c*) H. R. Kricheldorf and A. Stricker, *Macromol. Chem. Phys.*, 1999, **200**, 1726-1733; (*d*) M. H. Chisholm, J. C. Gallucci and C. Krempner, *Polyhedron*, 2007, **26**, 4436-4444; (*e*) A. Grafov, S. Vuorinen, T. Repo, M. Kemell, M. Nieger and M. Leskela, *Eur. Polym. J.*, 2008, **44**, 3797-3805.

4 (*a*) G. Labourdette, D. J. Lee, B. O. Patrick, M. B. Ezhova and P. Mehrkhodavandi, *Organometallics*, 2009, **28**, 1309-1319; (*b*) W.-C. Hung, Y. Huang and C.-C. Lin, *J. Polym. Sci., Part A: Polym. Chem.,* 2008, **46**, 6466-6476; (*c*) J. Borner, S. Herres-Pawlis, U. Florke and K. Huber, *Eur. J. Inorg. Chem.,* 2007, 5645-5651; (*d*) S. D. Bunge, J. M. Lance and J. A. Bertke, *Organometallics,* 2007, **26**, 6320-6328; (*e*) H.-Y. Chen, H.-Y. Tang and C.-C. Lin, *Macromolecules*, 2006, **39**, 3745-3752; (*f*) E. Bukhaltsev, L. Frish, Y. Cohen and A. Vigalok, *Org. Lett.,* 2005, **7**, 5123-5126. (*g*) H.-Y. Chen, B.-H. Huang and C.-C. Lin, *Macromolecules*, 2005, **38**, 5400-5405; (*h*) C.-M. Che and J.-S. Huang, *Coord. Chem. Rev.*, 2003, **242**, 97-113; (*i*) T. R. Jensen, L. E. Breyfogle, M. A. Hillmyer and W. B.Tolman, *Chem. Commun.*, 2004, 2504-2505. (*g*) R. Tong and J. Cheng, *Angew. Chem. Int. Ed.,* 2008, **47**, 4830-4834; (*k*) K. Yu and C. W. Jones, *J. Catal.,* 2004, **222**, 558; (*l*) M. Helou, O. Miserque, J.-M. Brusson, J.-F. Carpentier and S. M. Guillaume, *Macromolecul. Rapid Commun.,* 2009, **30**, 2128-2135; (*m*) X. Xu, Y. Chen, G. Zou, Z. Ma and G. Li, *Journal of Organometallic Chemistry*, 2010, **695**, 1155-1162.

5 (*a*) T. J.J. Whitehorne, B. Varbe and F. Schaper, *Dalton Trans.,* 2014, **43**, 6339-6352; (*b*) R. Petrus and P. Sobota, *Organometallics*, 2012, **31**, 4755-4762; (*c*) C. C. Roberts, B. R. Barnett, D. B. Green and J. M. Fritsch, *Organometallics* 2012, **31**, 4133-4141; (*d*) B.-H. Huang, C.-N. Lin, M.-L. Hsueh, T. Athar and C.-C. Lin, *Polymer*, 2006, **47**, 6622-6629; (*e*) R. Qi, B. Liu, X. Xu, Z. Yang, Y. Yao, Y. Zhang and Q. Shen, *Dalton Trans*., 2008, 5016-5024; (*f*) S. Bhunora, J. Mugo, A. Bhaw-Luximon, S. Mapolie, J. Van Wyk, J. Darkwa and E. Nordlander, *Appl. Organometal. Chem*., 2011, **25**, 133-145; (*g*) D. Darensbourg and O. Karroonnirun, *Inorg. Chem.,* 2010, **49**, 2360-2371.

6 N. M. Rezayee, K. A. Gerling, A. L. Rheingold and J. M. Fritsch, *Dalton Trans*., 2013, **42**, 5573-5586.

7 **7** X.-F. Yu, C. Zhang and Z.-X. Wang, *Organometallics*, 2013, **32**, 3262-3268.

8 (*a*) E. Grunova, T. Roisnel and J.-F. Carpentier, *Dalton Trans*., 2009, **41**, 9010-9019; (*b*) K. A. Gerling, N. M. Rezayee, A. L. Rheingold, D. B. Green and J. M. Fritsch, *Dalton Trans*., 2014, **43**, 16498.

9 W. C. Hung, Y. Huang and C. C. Lin, *J. Polym. Sci., Part A: Polym. Chem.,* 2008, **46**, 6466

10 (*a*) M. Cheng, A. B. Attygalle, E. B. Lobkovsky, and G. W. Coates, *J. Am. Chem. Soc.,* 1999, **121**, 11583-11584; (*b*) Scott D. Allen, D. R. Moore, E. B. Lobkovsky and G. W. Coates, *Journal of Organometallic Chemistry*, 2003, **683**, 137-148; (*c*) M. Cheng, D. R. Moore, J. J. Reczek, B. M. Chamberlain, E. B. Lobkovsky and Geoffrey W. Coates, *J. Am. Chem. Soc.,* 2001, **123**, 8738-8749; (*d*) L. R. Rieth, D. R. Moore, E. B. Lobkovsky and Geoffrey W. Coates, *J. Am. Chem. Soc.,* 2002, **124**, 15239-15248; (*e*) D. R. Moore, M. Cheng, E. B. Lobkovsky and Geoffrey W. Coates, *J. Am. Chem. Soc.,* 2003, **125**, 11911-11924; (*f*) C. M. Byrne, S. D. Allen, E. B. Lobkovsky and Geoffrey W. Coates, *J. Am. Chem. Soc.,* 2004, **126**, 11404-11405; (*g*) E. W. Dunn and Geoffrey W. Coates, *J. Am. Chem. Soc.,* 2010, **132**, 11412-11413; (*h*) D. R. Moore, M. Cheng, E. B. Lobkovsky and G. W. Coates, *Angew. Chem. Int. Ed.,* 2002, **14**, 41.

11 N. M. Rajendran, A. Haleel and N. Dastagiri Reddy, *Organometallics*, 2014, **33** 217-224.

12 (*a*) O. S. Trofymchuk, D. V. Gutsulyak, C. Quintero, M. Parvez, C. G. Daniliuc, W. E. Piers and R. S. Rojas, *Organometallics,* 2013, **32** (**24**), 7323-7333; (*b*) O. S. Trofymchuk, G. B. Galland, M. A. Milani, and R. S. Rojas, *J. Polym. Sci. A Polym. Chem.*, 2014, doi: 10.1002/pola.27456.

13 (*a*) M. H. Chisholm, J. C. Gallucci and Khamphee Phomphrai, *Inorg. Chem.,* 2005, **44**, 8004-8010; (*b*) A. P. Dove, V. C. Gibson, E. L. Marshall, A. J. P. White and D. J. Williams, *Dalton Trans.*, 2004, 570-578.

14 (*a*) *J. D. Azoulay, R.* S. *Rojas, A. V. Serrano*, H. Ohtaki, G. B. Galland and G. Wu, *Angew. Chem. Int. Ed.,* 2009, **48**, 1089-1093.(*b*) *A. R. Cabrera*, Y. Schneider, M. Valderrama, R. Frohlich, G. Kehr, G. Erker and R. S. Rojas, *Organometallics,* 2010, **29**, 6104-6110; (c) *B. M. Boardman*, J. M. Valderrama, F. Muñoz, G. Wu, G. C. Bazan and R. Rojas, *Organometallics,* 2008, **27**, 1671-1674; (d) *R. Bisatto*, G. B. Galland, R. Rojas and G. Bazan, *J. Polym. Sci. Part A: Polym. Chem.,* 2008, **46**, 54-59; (e) R. S. Rojas, J. Wasilke, G. Wu, J. Ziller and G. C. Bazan, *Organometallics,* 2005, **24**, 5644-5653; (f) S. L. Scott, B. C. Peoples, C. Yung, R. S. Rojas, V. Khanna, H. Sano, T. Suzukie and F. Shimizue, *Chem. Commun*., 2008, 4186-4188; (*g*) B. C. Peoples, R. Rojas, *Olefin Upgrading Catalysis*, 2011, 39-75.

15 (*a*) H. Jacobsen, H. Berke, S. Döring, G. Kehr, G. Erker, R. Fröhlich and O. Meyer, *Organometallics*, 1999, **18**, 1724-1735; (*b*) C. Herrmann, G. Kehr, R. Fröhlich and G. Erker, *Organometallics*, 2008, ***27***, 2328-2336.

16 (*a*) K. Spannhoff, R. Rojas, R. Frohlich, G. Kehr and G. Erker, *Organometallics*, 2011, **30**, 2377-2384 (*b*) D. J. Parks, R. E. v H. Spence and W. E. Piers*, Angew. Chem., Int. Ed.*, 1995, **107**, 895-897; (*c*) D. J. Parks, R. E. v H. Spence and W. E. Piers*, Angew. Chem., Int. Ed.,* 1995, **34**, 809-811. (*d*) D. J. Parks, W. E. Piers and G. P. A. Yap, *Organometallics*, 1998, **17**, 5492-5503.

17 (*a*) D. A. Walker, T. J. Woodman, D. L. Hughes and M. Bochmann, *Organometallics,* 2001, **20***,* 3772-3776; (*b*) N. Kotzen, I. Goldberg and A. Vigalok, *Organometallics,* 2009, **28***,* 929-932; (*c*) J. Klosin, G. R. Roof, E. Y.-X. Chen and K. A. Abboud, *Organometallics,* 2000, **19**, 4684-4686.

18 (*a*) P. Jochmann and D. W. Stephan, *Organometallics*, 2013, **32**, 7503-7508; (*b*) S. Aboulkacem, W. Tyrra and I. Pantenburg, *Z. Anorg. Allg. Chem.,* 2003, **629**, 1569-1574.

19 K. Pang, Y. Rong and G. Parkin, *Polyhedron*, 2010, **29**, 1881-1890.

20 (*a*) B. M. Chamberlain, M. Cheng, D. R. Moore, T. M. Ovitt, E. B. Lobkovsky and G. W. Coates, *J. Am. Chem. Soc.,* 2001, **123***,* 3229-3238; (*b*) G. Schnee, C. Fliedel, T. Aviles and S. Dagorne, *Eur. J. Inorg. Chem.*, 2013, **21**, 3699-3709.

21 Z. Liu, W. Gao, J. Zhang, D. Cui, Q. Wu and Y. Mu, *Organometallics*, 2010, **29**; 5783-5790.

22 P. Dubois, C. Jacobs, R. Jerome and P. Teyssie, *Macromolecules***,** 1991, **24** (9), 2266-2270.

23 (*a*) H. R. Kricheldorf, M. Berl and N. Scharnagl, *Macromolecules,* 1988, **21** (2), 286-293; (b) V. T. Lipik, L. K. Widjaja, S. S. Liow, M. J. M. Abadie and S. S. Venkatraman, *Polym. Degrad. Stab.* 2010, **95** (12), 2596-2602.